Available online at www.sciencedirect.com
SCIENCE DIRECT
Journal of the European Ceramic Society 26 (2006) 901–908
www.elsevier.com/locate/jeurceramsoc

Study of the preparation conditions for $NiMn_2O_4$ grown from hydroxide precursors

G. Ashcroft[a], I. Terry[b,*], R. Gover[c,1]

[a] *National Physical Laboratory, Teddington, UK*
[b] *Department of Physics, Science Laboratories, South Road, University of Durham, Durham, UK*
[c] *Department of Chemistry, Science Laboratories, South Road, University of Durham, Durham, UK*

Received 30 June 2004; received in revised form 22 November 2004; accepted 26 November 2004
Available online 21 January 2005

Abstract

An investigation of mixed oxide route preparation routes for nickel manganite has confirmed that residual nickel oxide is present regardless of the particular conditions adopted [Wickham, D. G., Solid-phase equilibria in the system $NiO–Mn_2O_3–O_2$. *J. Inorg. Nucl. Chem.*, 1964, **26**, 1369–1377; de Gyorgyfalva, G. D. C. C., Nolte, A. N. and Reaney, I. M., Correlation between microstructure and conductance in NTC thermistors produced from oxide powders. *J. Eur. Ceram. Soc.*, 1999, **19**, 857–860]. The co-precipitation of mixed hydroxides of nickel and manganese was successfully employed to eliminate any unreacted nickel oxide remaining after firing, though the requirements for single phase nickel manganite were investigated in detail and found to be quite stringent. Synthesized materials were characterized by X-ray powder diffraction measurements with diffraction patterns being analysed using the Rietveld technique. A systematic investigation into the optimum firing conditions confirmed that a minimal impurity content is achieved in samples rapidly heated to 800 °C, and fired for at least 48 h. Nickel oxide was found to be the dominant impurity phase at higher firing temperatures.

Keywords: Powders-solid state reaction; X-ray methods; Spinels; $NiMn_2O_4$

1. Introduction

Nickel manganite has found widespread use as a material for negative temperature coefficient (NTC) thermistor devices.[2,3] The material is ferrimagnetic, has a spinel structure[4] and, in common with many other spinels, it has a partially inverse structure;

$$Mn_\nu Ni_{1-\nu}[Ni_\nu Mn_{2-\nu}]O_4$$

where ν is the degree of inversion. The degree of inversion determines both the electrical[3,5,6] and magnetic properties[1] of $NiMn_2O_4$ and thus it is important to be able to control this parameter if reproducible material for devices is to be fabricated. There have been many investigations into the properties of nickel manganite using a wide range of preparation routes and characterisation techniques. The variability in reported material properties[2,7,8] suggests problems with sample purity in many previous investigations. The temperature range over which $NiMn_2O_4$ is believed to be stable has decreased[1,4,9] with the advent of high resolution diffraction, Rietveld analysis and thermogravimetry. In many cases the published data is not sufficient to determine the quality of the samples used and so it is difficult to determine which of the range of reported characteristics are those of pure $NiMn_2O_4$. Therefore, the goal of the present work was to adopt a successful method for producing samples of $NiMn_2O_4$ and establish the conditions for producing the purest possible material. A detailed investigation into the magnetic properties

* Corresponding author. Tel.: +44 191 334 3725; fax: +44 191 334 5823.
E-mail address: ian.terry@durham.ac.uk (I. Terry).
[1] Present address: Advanced Research Laboratory, Valence Technology Building 62, Rissington Business Park, Upper Rissington, Gloucestershire, UK.

0955-2219/$ – see front matter © 2004 Elsevier Ltd. All rights reserved.
doi:10.1016/j.jeurceramsoc.2004.11.023

of such pure material will be described in a subsequent paper.

2. Experimental

The mixed oxide route has been used by a number of authors to produce nickel manganite (for example, see[2]). A preliminary investigation was carried out using this route with stoichiometric amounts of MnO_2 and NiO being mechanically mixed, fired for 12 h at 1200 °C, and annealed at 800 °C for 60 h.[10] Unfortunately, all samples of $NiMn_2O_4$ produced by this method were contaminated by NiO as evidenced by high resolution X-ray diffraction measurements. This is believed to be due to the incomplete mixing of the precursor oxides, and low mobility of the metal atoms at 800 °C. Raising the firing temperature to 1200 °C, in order to speed up the reaction, caused NiO to segregate out of nickel manganite, and it was found to show little tendency to be re-absorbed by annealing at 800 °C.[6] Therefore the mixed oxide route was found to be unsuitable to make pure $NiMn_2O_4$, confirming previous findings.[1,2] However, Macklen[11] has found it possible to reduce the residual NiO impurity by repeated firing and grinding. Other routes involving mechanical mixing of solid precursors (carbonates,[12] nitrates[13]) would be expected to suffer from the same problems as the oxide route. The oxalate route[1,3,14] has been used successfully to produce $NiMn_2O_4$ via an intermediate defect spinel phase in a two-stage firing process. Reported problems with the tendency of manganese oxalate to form supersaturated solutions[1] have been overcome by various methods.[1,3]

The hydroxide route [7,15] has been successful in producing intimately mixed nickel and manganese precursors suitable for preparing $NiMn_2O_4$. In the present work the starting materials were the tetra-hydrated acetates $Ni(CH_3CO_2)_2{\cdot}4(H_2O)$ and $Mn(CH_3CO_2)_2{\cdot}4(H_2O)$, quoted purity >99%, which were obtained from Aldrich Chemicals. The weighed acetates were dissolved in distilled water, and a slight excess of sodium hydroxide solution was slowly added in order to ensure complete precipitation. The resulting mixture was stirred for a further 4–8 h, and then suction filtered. The filtrate was repeatedly washed with distilled water to remove any remaining sodium acetate or unreacted sodium hydroxide, dried at 120 °C overnight, ground, washed with distilled water, and dried overnight again. An X-ray diffraction pattern of the resulting intimately mixed hydroxides showed the absence of any well-defined Bragg reflections,[10] indicating either an extremely small crystal size, or an amorphous sample. In either case, a high reactivity was expected. The initial batch of samples of $NiMn_2O_4$ were prepared at a variety of firing temperatures, and were heated at a rate of 10 °C min^{-1}, held at the required temperature for 20 h, then removed from the furnace and left to cool to room temperature.

In addition, the firing schedule as used by the oxide route (firing at 1200 °C followed by an extended anneal at 800 °C) was used with hydroxide precursors.[10] The resulting sample showed no evidence of a NiO phase present, but the nickel manganite phase was significantly nickel deficient. The non-stoichiometry produced by this firing schedule precludes its use for producing high quality samples.

X-ray diffraction was used to identify any impurities present, and to confirm the crystal structure of $NiMn_2O_4$.[1,6] The limit of detection for crystalline impurity phases was expected to be 1–3%. All X-ray diffraction data were taken using a Siemens D5000 diffractometer fitted with a copper X-ray tube, and the data were collected in the range $10° \leq 2\theta \leq 120°$, with a step size of 0.02°. All of the patterns were recorded over a period of 12 h, and the height of the most intense peak ranged from approximately 5000 to 16,000 counts. The diffraction data were analysed by the Rietveld technique[16] using the computer programs, FULLPROF, and WinPLOTR.[17] Validation of the Rietveld technique was achieved by generating simulated datasets using FULLPROF, and then subjecting them to Rietveld analysis in a similar manner to the real data collected.[10]

Scanning electron micrographs were obtained using a JEOL, JSM-IC848 SEM with an EDX head for the analysis of fluorescence from the material.

3. Results and discussion

3.1. X-ray diffraction

X-ray diffraction patterns of nickel manganite produced at temperatures between 600 and 1100 °C are shown in Fig. 1. Sinha et al.,[4] and many others gave the space group of $NiMn_2O_4$ as *Fd*3*m*, and lattice parameter as approximately 8.4 Å, and the X-ray pattern corresponding to this structure can be seen in all traces shown in Fig. 1. However, samples fired at 780 °C and below show additional diffraction peaks present that can be accounted for by the reflections from α-Mn_2O_3,[18] Mn_3O_4,[19] and $NiMnO_3$.[20] Thus it can be concluded that at 780 °C the reaction had not gone to completion. It was expected that 800 °C would be close to the optimum firing temperature for the production of pure $NiMn_2O_4$.[6,8] Crystallinity improves in the samples fired at higher temperatures, with well-defined peaks at all angles, indicating that the relevant reactions have proceeded to a point approaching thermodynamic equilibrium. Scanning electron micrographs also reveal the sample fired at higher temperature is much more densely sintered with a larger grain size. NiO was a possible impurity phase at high temperatures (above 900 °C),[21] however the expected diffraction patterns from this, and $NiMn_2O_4$, have a large amount of overlap and the quality of the material can only be assessed with a detailed Rietveld analysis of the diffraction patterns. Nevertheless, visual inspection of the 1100 °C dataset reveals that nickel oxide (NiO[22]) has segregated out of the sample and a nickel-deficient spinel has been formed. This is expected from a published phase diagram,[1] which shows the region of temperature in which the spinel is stable increases with spinel

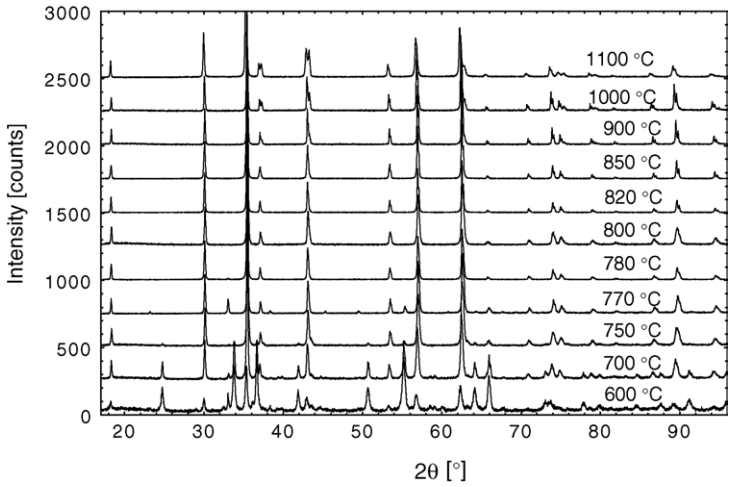

Fig. 1. X-ray diffraction patterns observed from samples fired at temperatures of 600–1100 °C. All the datasets have been normalised to an intensity of 1000 for the strongest peak, and are offset for clarity.

manganese concentration. The NiO peaks are narrower than the spinel peaks at a similar scattering angle, implying the formation of larger crystallites and, perhaps, an increase in strain within the nickel manganite. The tendency for these NiO crystallites to be re-absorbed at a lower temperature is probably low, as the nickel would have to then diffuse a considerable distance in order to establish a homogenous distribution. Therefore, annealing such a material at, say, 800 °C would fail to produce stoichiometric nickel manganite even when annealing times are long.

Analysing the X-ray diffraction patterns with the Rietveld technique began by fixing the inversion parameter at a value of 0.8, which was representative of those previously reported.[1,8,23–25] Fixing the inversion parameter was not believed to have a large effect on the calculated intensities, as the contrast in the form factors of nickel and manganese is small. The other fitting parameters were turned-on in a sequence in accord with that suggested by Young.[26] Various impurities already identified as being present were included as additional phases in the refinements where appropriate. Results from all of the Rietveld refinements, are to be found in reference 10 and a portion of a fit is shown in Fig. 2 for a sample fired at 800 °C. Close inspection of the plotted difference between the data, and calculated fit for the sample fired at 800 °C reveals several features with the obvious discrepancies between the data and fit at $2\theta = 37.4°$, 43.4°, and 75.5° (not shown in Fig. 2) corresponding to diffraction peaks from NiO. Therefore, NiO was included as a second phase in the model used for Rietveld refinement of this, and the other datasets. Sasaki et al.,[22] gave the space group of NiO as *Fm*3*m*, and a lattice parameter of 4.178(1) Å. The profile coefficients of the NiO phase were set the same as those of $NiMn_2O_4$, and the lattice parameter of NiO was not refined. The discrepancies were eliminated almost entirely by the addition of a NiO phase to the Rietveld refinement model (Fig. 2b), and the *R* values, and goodness of fit indicator also fell significantly as a result of this (Table 1). A plot of the final fitted data, and error on the fit is given in Fig. 3. Note that the lattice parameter, and the oxygen parameter, were significantly underestimated when

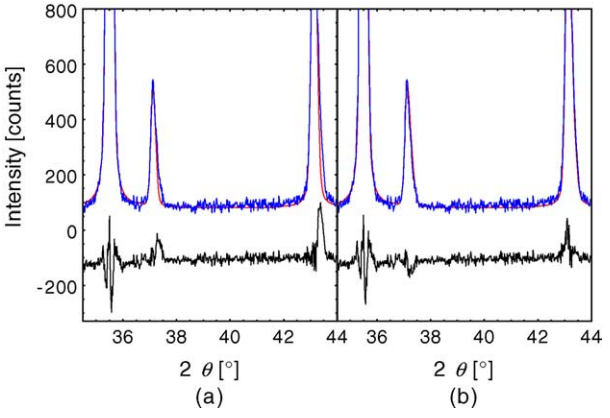

Fig. 2. Detail of the data from the sample fired at 800 °C, and fit to this data before, and after inclusion of a NiO phase, and plots of the difference between the data and fit. This latter curve has been offset for clarity.

Table 1
Results from the Rietveld refinement of the data from the sample fired at 800 °C before, and after inclusion of a NiO phase

	Before	After
Scale ($NiMn_2O_4$) × 10^4	1.528(10)	1.4930(84)
Scale (NiO) × 10^4	0	1.399(77)
U	0.115(14)	0.120(11)
V	0.046(12)	0.353(97)
W	0.0042(23)	0.0063(20)
η_0	0.351(30)	0.371(25)
η_1	0.00256(57)	0.00151(48)
x (O)	0.26407(17)	0.26418(17)
B (8a)	0.554(26)	0.558(26)
B (16d)	0.373(21)	0.375(21)
B (32e)	0.827(54)	0.835(53)
R_p	5.96	5.91
R_{wp}	8.27	8.25
S	1.29	1.23

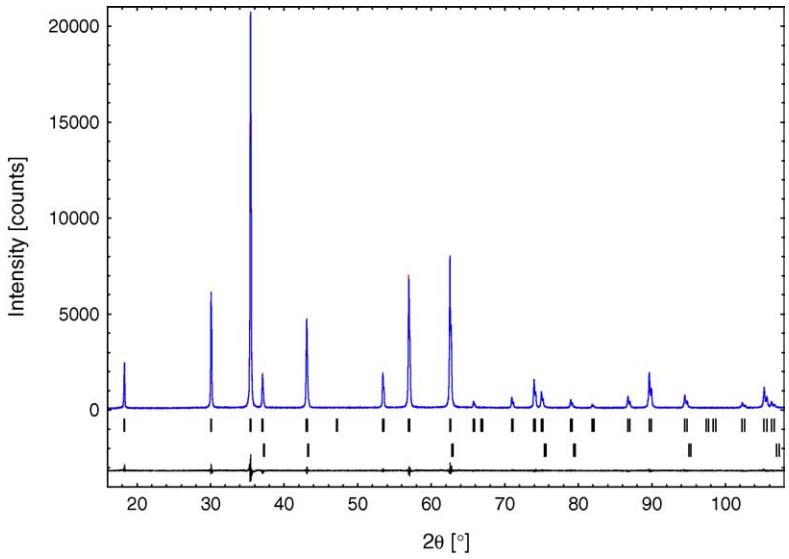

Fig. 3. X-ray diffraction data collected on the sample fired at 800 °C, and a fit to the data using the Rietveld technique. The difference curve has been offset for clarity. The upper line of marked reflections correspond to the structure of $NiMn_2O_4$ and the lower line to that of NiO.

NiO was present in a sample, but not accounted for in the Rietveld refinement. Unfortunately, this represents the most likely scenario for much of the previous reported diffraction studies of $NiMn_2O_4$ as only one report (Wickham[1]) specifically mentions the inclusion of NiO as an impurity phase when refinements were carried out, and this was not by the Rietveld method.

3.2. Results from Rietveld refinement

3.2.1. Growth temperature

The amount of NiO contamination found in the samples, and the variation in the lattice parameter of $NiMn_2O_4$ with firing temperature, are shown in Fig. 4. NiO contamination appears to be at its lowest in the samples fired around 800 °C, and there is a minimum in the lattice parameter of $NiMn_2O_4$, centred on approximately 800 °C, which coincides with the region of lowest impurity content. The values of lattice parameter determined for the purest samples agree well with many previously reported values. However, the samples fired at $T > 800$ °C, which show an increasing NiO contamination, have a $NiMn_2O_4$ lattice parameter that increases with impurity content. $NiMn_2O_4$ may be nickel deficient above the temperature region where relatively pure samples were found. If the majority of nickel in $NiMn_2O_4$ is Ni^{2+}, then a nickel deficiency will result in a corresponding increase in the amount

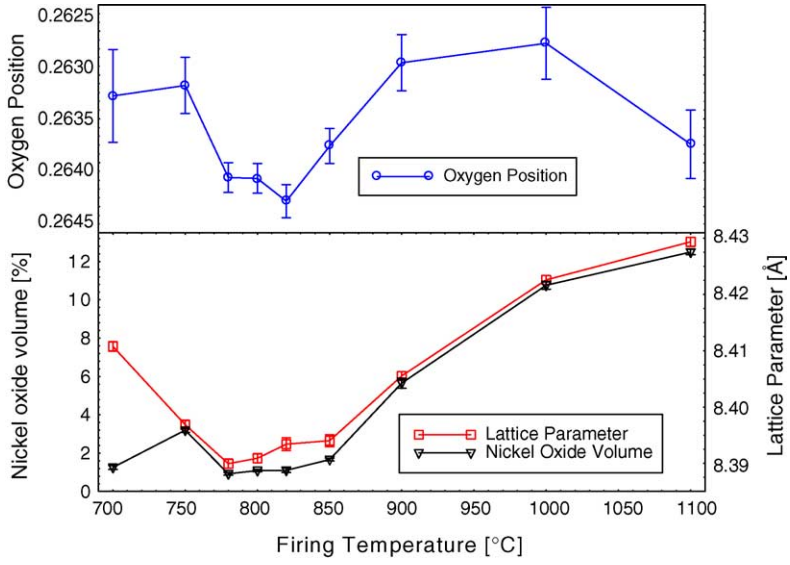

Fig. 4. Refined lattice parameter of $NiMn_2O_4$, amount of NiO present, and oxygen position parameter in samples fired at various temperatures for 20 h. The error bars for the lower graph are equal to, or smaller than the size of data points. Note that the error bars represent only the statistical error reported from the fitting procedure, and do not take into account any systematic errors that may be present.

of Mn^{2+} present, which has a larger radius, and an increased lattice parameter would be expected. This is corroborated by Larson et al.,[6] in a study of the $Ni_{(1-x)}Mn_{(2+x)}O_4$ system, and implies that the samples of those authors who have reported an usually large lattice parameter for $NiMn_2O_4$[7] may have been non-stoichiometric. Larson et al.,[6] also observed a large distortion to tetragonal symmetry for values of x greater than 0.42. Since no peak splitting was observed in the data of Fig. 1, $x = 0.42$ can be considered a lower limit on the amount of nickel present in the spinel phase. Assuming that no metal was lost from the samples during preparation (which is expected given that the melting points of all materials were greater than 1100 °C), this implies an upper limit of 13.5% (volume) on the amount of NiO present. The only sample approaching this limit was fired at 1100 °C, which contained 12.49(14)% NiO, corresponding to a nickel deficiency of $x = 0.389(4)$.

Of the impurity phases identified in samples fired at temperatures below 800 °C, the most abundant (27.29(42)% at 700 °C) is $NiMnO_3$. This structure is believed[1] to accommodate a considerable amount of non-stoichiometry, undetectable by analysis of X-ray powder diffraction data. It is suggested that the actual impurity phase present at lower temperatures is $Ni_{(1-\beta)}Mn_{(1+\beta)}O_3$ with $0 \leq \beta \leq 1/3$. This, in combination with the spinel, NiO, and a small amount of α-Mn_2O_3 (as reported by Feltz et al.[14] and Drouet et al.[27]), allows the correct overall nickel to manganese ratio to be preserved in the low temperature samples.

The variation of the refined oxygen position parameter with changes in firing temperature is shown in Fig. 4. The values are slightly higher than most of those previously reported, but nearer to those values predicted for the case of high spin manganese ions (as detailed in ref.[10]). Validation testing of the FULLPROF refinement program indicated that the presence of NiO reflections caused the refined value of the oxygen position parameter to be underestimated, which could account for the observed dependence upon firing temperature and therefore impurity content. The slight discrepancy with previous reports could be due to a similar systematic underestimation of the oxygen parameter in earlier Rietveld refinements, which did not include the presence of NiO.[7,8,23,25,28] It has been noted that the presence of NiO implies a nickel deficiency in $NiMn_2O_4$, and therefore a change in the average ionic size of the ions in the A and B sites. The oxygen parameter is sensitive to the difference in the sizes of the ions, with an increase in oxygen parameter being caused by an increase in the size of the A site, or a decrease in size of the B site. Using the ionic radii given in refs.[29,30] and the cation distribution postulated by Brabers,[31] it is predicted that an increase in oxygen parameter would result if Ni^{2+} was preferentially lost from the A sites, to be replaced by the much larger Mn^{2+} ion. The increase in oxygen position parameter in the sample fired at 1100 °C, where proportion of nickel lost to NiO in the sample was considerable (see Fig. 4), supports this prediction.

The isotropic temperature factors (or B factors) of the various sites, obtained from Rietveld refinements are shown in Fig. 5. The 8a, 16d, and 32e sites correspond to A sites, B sites, and oxygen positions, respectively. The oxygen B values are high, as has been observed previously[32] and may be expected because of the smaller oxygen mass compared to the cations. It should be noted that X-ray diffraction is not particularly sensitive to oxygen, and therefore neutron diffraction measurements are necessary to confirm the high values of B shown in Fig. 5. However, the existence of such high values of B was postulated to be partly due to local Jahn-Teller type distortions (which are non co-operative for low concentrations of Mn^{3+}, the Jahn-Teller active ion). Thus the increase of the oxygen B values with increasing firing temperature may be due to an increase in the proportion of the B sites occupied by Mn^{3+} ions. This is in accordance with reports of the cation distribution,[33,34] and the change in inversion pa-

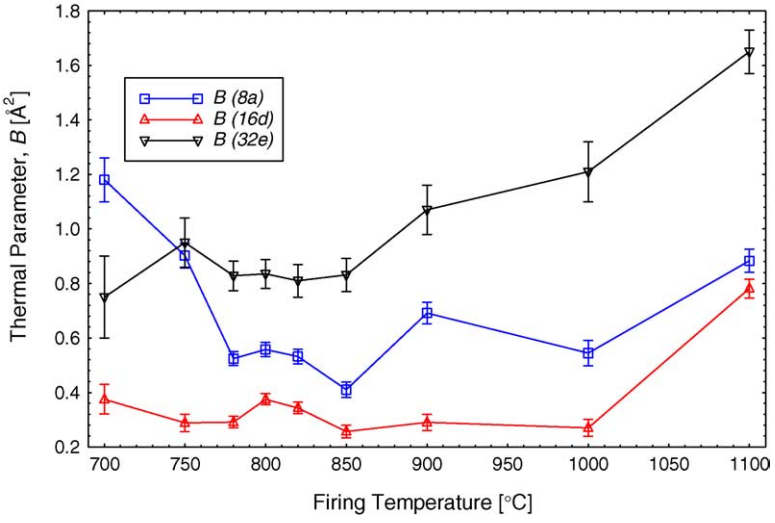

Fig. 5. Refined isotropic temperature factors for $NiMn_2O_4$ for samples fired at various temperatures.

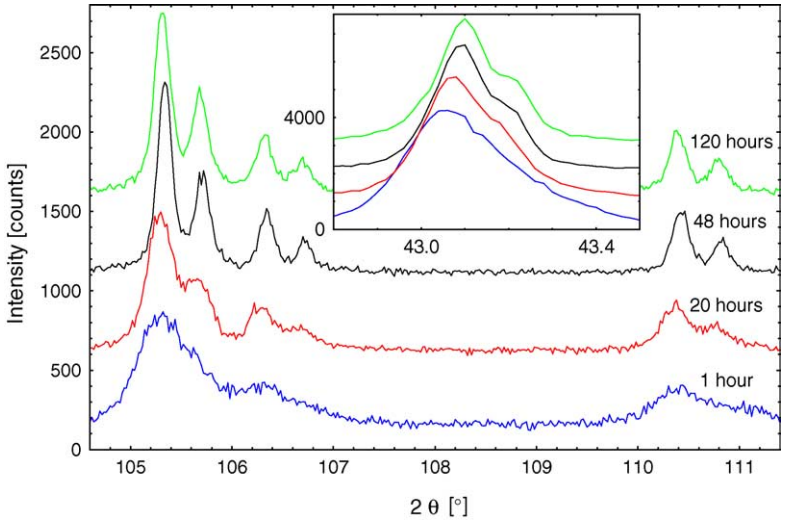

Fig. 6. Detail of the X-ray diffraction patterns observed from samples fired for between 1 and 120 h at 800 °C. The datasets have been offset for clarity.

rameter with temperature.[11,28] Also, any loss of nickel from $NiMn_2O_4$ (for example, by the segregation of NiO) will act to increase the amount of the B sites occupied by Mn^{3+}. However, it should be noted that the systematic rise in *B* factors with firing temperature above 900 °C may be possibly related to an over-estimation of the intensities of some of the $NiMn_2O_4$ diffraction peaks that overlap with NiO diffraction peaks.

3.2.2. Firing time

A number of samples were prepared at 800 °C with firing times varying between 1 and 120 h. The X-ray diffraction patterns obtained from these samples were similar with only the data from the sample fired for 1 h showing an extra small peak which is attributed to the strongest [2 2 2] reflection from α-Mn_2O_3. Closer inspection of the data (see Fig. 6) shows that changing the firing time mainly changes the peak widths. Also, the (2 2 2) and (4 0 0) peaks (shown in Fig. 6, inset) reveal a decrease in peak asymmetry as the firing time is extended. This asymmetry is again attributed to the presence of the (1 1 1), and (2 0 0) reflections of NiO at $2\theta = 37.3^\circ$ and $2\theta = 43.3^\circ$, respectively. However, there is no indication of any significant amounts of NiO in the samples fired for 48, and 120 h. Also, the $K_{\alpha1}$, $K_{\alpha2}$ splitting of the incident radiation is evident from the shape of the peaks from the samples fired for 48, and 120 h, indicating a higher crystallinity in these samples

Rietveld analysis was carried out on these datasets and the variation in refined lattice parameter, and amount of NiO present is shown in Fig. 7. There is a small, but statistically

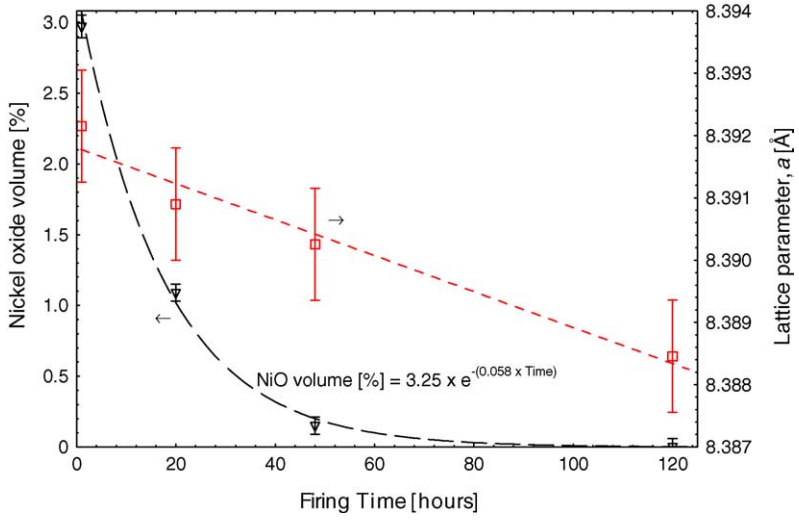

Fig. 7. Amount of NiO present, and refined lattice parameter of $NiMn_2O_4$, in samples fired for various times at 800 °C. The lattice parameter error bars represent an estimate of the total combined uncertainty, in accordance with UKAS, and BIPM guidelines, while the NiO amount error bars represent only the statistical error reported from the fitting procedure, and do not take into account any systematic errors that may be present. The dashed lines are fits to the data, with the NiO amount fitted to an exponential decay, and a linear fit to the lattice parameter.

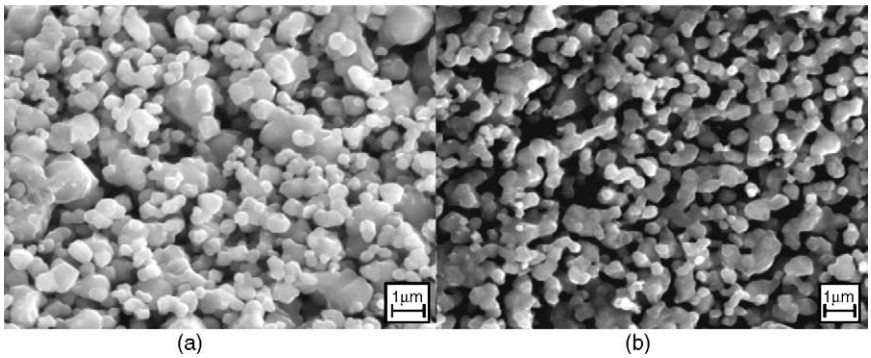

Fig. 8. SEM images of $NiMn_2O_4$ prepared at 800 °C for 48 h with a heating rate of (a) 1 K min^{-1} and (b) 10 K min^{-1}.

significant decrease in lattice parameter with increasing firing time, and the correlation between lattice parameter and amount of NiO is similar to that observed for samples with differing firing temperatures (Fig. 4). Therefore, the mechanism for the change in lattice parameter was assumed to be related to nickel deficiency in samples fired for short times. The isotropic temperature factors (*B* factors) of the various sites, obtained from Rietveld refinements are broadly consistent from sample to sample, and agree well with other samples fired at temperatures around 800 °C. It is clear that the samples which were fired for 48 and 120 h had the highest purities, and it was concluded that 48 h was an adequate firing time to produce well crystallised material. This conclusion was supported by SEM micrographs of the samples, where grain size was noticeably larger in the sample fired for 48 h (typically ∼100 nm), than it was in the sample fired for 20 h (typically ∼500 nm), yet there was no significant increase in grain size when the firing time was further increased to 120 h.

3.2.3. Heating rate

The experiments carried out at different firing temperatures have demonstrated that single phase $NiMn_2O_4$ cannot be produced below a preparation temperature of approximately 800 °C. This confirms earlier reports in the literature[3,6] where it was concluded that rapid heating to, and cooling from, the sample firing temperature is conducive to high sample purity. To test this supposition, a sample was prepared using a heating rate of 1 °C min^{-1} to 800 °C, and held there for 48 h. The only diffraction peak not an expected reflection from $NiMn_2O_4$, was attributed to the strongest (2 2 2) reflection from α-Mn_2O_3, indicating that the reaction to produce $NiMn_2O_4$ had not proceeded to completion in this sample. This may be due to α-Mn_2O_3 forming large crystals while the sample was being heated to 800 °C, and the manganese then only slowly diffusing to form $NiMn_2O_4$. A SEM micrograph of this sample is shown in Fig. 8a, revealing the presence of occasional larger crystals, in contrast to the sample with a higher heating rate, Fig. 8b. Thus the maximum heating rate available (10 °C min^{-1}) was used when synthesising pure $NiMn_2O_4$.

4. Summary

The conditions for the production of pure $NiMn_2O_4$ from hydroxide precursors have been studied. The mixed oxide route was found to be unsuitable to produce pure material, while the hydroxide route, using coprecipitated precursor material, has been shown to result in single phase material as a consequence of the small particle size of these precursors. The optimum preparation temperature was investigated in the region 600–1100 °C, with a minimum in the lattice parameter coinciding with minimal impurity content at 800 °C. Samples fired at 780 °C and below show evidence for a mixed material with α-Mn_2O_3, Mn_3O_4, and $NiMnO_3$ detected, and it can be concluded that in these specimens the reaction did not go to completion. Above 800 °C the dominant impurity is NiO which increases in concentration as the firing temperature increases. Lattice parameter and oxygen parameter values for the samples of $NiMn_2O_4$ were found to agree well with previously reported values. The effect of varying the firing time and heating rate were investigated, and findings were that impurity content decreased with increasing firing time at 800 °C, and a slow heating rate gave rise to an increased amount of α-Mn_2O_3. A firing time of 48 h was found to be an adequate for the production of high quality nickel manganite, and the maximum heating of 10 °C min^{-1} was shown to also be essential to minimise impurity level.

Validation of the Rietveld technique applied to diffraction patterns was carried out using simulated datasets and highlighted significant errors in the fitting parameters when NiO impurities were present but not accounted for. Such a situation gives estimates of lattice parameter and oxygen parameter that are much too low. This highlights the need for careful Rietveld analysis of the diffraction data of nickel manganite when determining the suitability of all growth methods of this important material.

Acknowledgements

We thank Dr. J.S.O. Evans for the use of X-ray diffraction facilities, and Dr. K. Durose and Dr. A. Yates for providing us

with access to the scanning electron microscope. G. Ashcroft gratefully acknowledges financial support from the EPSRC.

References

1. Wickham, D. G., Solid-phase equilibria in the system NiO–Mn_2O_3–O_2. *J. Inorg. Nucl. Chem.*, 1964, **26**, 1369–1377.
2. de Gyorgyfalva, G. D. C. C., Nolte, A. N. and Reaney, I. M., Correlation between microstructure and conductance in NTC thermistors produced from oxide powders. *J. Eur. Ceram. Soc.*, 1999, **19**, 857–860.
3. Schmidt, R., Stiegelschmidt, A., Roosen, A. and Brinkman, A. W., Screen printing of co-precipitated $NiMn_2O_{4+\delta}$ for production of NTCR thermistors. *J. Eur. Ceram. Soc.*, 2003, **23**, 1549–1558; Schmidt, R., Stiegelschmidt, A., Roosen, A. and Brinkman, A. W., Preparation and performance of thick film NTC thermistors. *Key Eng. Mater.*, 2002, **206–213**, 1417–1420.
4. Sinha, A. P. B., Sanjana, N. R. and Biswas, A. B., On the structure of some manganites. *Acta Cryst.*, 1957, **10**, 439–440.
5. Feltz, A., Topfer, J. and Neidicht, B., Investigations on electronically conducting oxide systems 23. Structure and properties of stable spinels in the series $M_zNiMn_{2-z}O_4$ (M = Li, Fe). *Z. Anorg. Allg. Chem.*, 1993, **619**, 39–46.
6. Larson, E. G., Arnott, R. J. and Wickham, D. G., Preparation, semiconduction and low temperature magnetisation of system $Ni_{1-x}Mn_{2+x}O_4$. *J. Phys. Chem. Solids*, 1962, **23**, 1771–1781.
7. Meenakshisundaram, A. *et al.*, Distribution of metal ions in transition metal manganites AMn_2O_4 (A: Co, Ni, Cu or Zn). *Phys. Status Solidi A*, 1982, **69**, 15–19.
8. Boucher, B., Buhl, R. and Perrin, M., Etude cristallographique du manganite spinelle cubique $NiMn_2O_4$ par diffraction de neutrons. *Acta Cryst. B*, 1969, **25**, 2326–2333.
9. Jung, J., Topfer, J. and Feltz, A., Thermoanalytical characterisation of $NiMn_2O_4$ formation. *J. Therm. Anal.*, 1990, **36**, 1505–1518.
10. Ashcroft, G. R., Ph.D. Thesis, Department of Physics, University of Durham, Durham, UK, 2003.
11. Macklen, E. D., Electrical conductivity and cation distribution in nickel manganite. *J. Phys. Chem. Solids*, 1986, **47**, 1073–1079.
12. Azaroff, L. V., Formation, structure and bonding of Ni–Co–Mn oxides having spinel-type structure. *Z. Kristallographie*, 1959, **112**, 33–43.
13. Renault, N., Baffier, N. and Huber, M., Cationic distribution and oxidation states in nickel manganites $NiMnO_4$ and $Ni_{0.8}Mn_{2.2}O_4$. *J. Solid State Chem.*, 1972, **5**, 250–254.
14. Feltz, A., Topfer, J. and Richter, U., Redox reactions in condensed oxide systems [XII] $NiMn_2O_4$ and $Ni_{1.5}Mn_{1.5}O_4$ in the metastable state and $NiMnO_3$ formation. *Eur. J. Solid State Inorg. Chem.*, 1994, **31**, 75–91.
15. Gillot, B. *et al.*, Phase transformation related kinetics in the oxidation of a manganese mixed-oxide with a spinel strucutre. *Mater. Chem. Phys.*, 1989, **24**, 199–208.
16. Rietveld, H. M., A profile refinement method for nuclear and magnetic structures. *J. Appl. Cryst.*, 1969, **2**, 65–71.
17. Roisnel, T. and Rodriguez-Carvajal, J., *Computer Program; WinPLOTR*. Laboratoire Leon Brillouin, Centre d'Etudes de Saclay, Gif-sur-Yvette, 2001.
18. Geller, S., Structures of α-Mn_2O_3, $(Mn_{0.983}Fe_{0.017})_2O_3$ and $(Mn_{0.37}Fe_{0.63})_2O_3$ and relation of magnetic ordering. *Acta Cryst. B*, 1971, **27**, 821–828.
19. Jarosch, D., Crystal structure refinement and reflectance measurements of hausmannite Mn_3O_4. *Mineral. Petrol.*, 1987, **37**, 15–23.
20. Cloud, W. H., Crystal structure and ferrimagnetism in $NiMnO_3$ and $CoMnO_3$. *Phys. Rev.*, 1958, **111**, 1046–1049.
21. de Gyorgyfalva, G. D. C. C. and Reaney, I. M., Decomposition of $NiMn_2O_4$ spinels. *J. Mater. Res.*, 2003, **18**, 1301–1308.
22. Sasaki, S., Fujino, K. and Takeuchi, Y., X-ray determination of electron density distribution in oxides MGO, MNO, CoO and NiO, and atomic scattering factors of their constituent atoms. *Proc. Jpn. Acad. B-Phys.*, 1979, **55**, 43–48.
23. Villers, G. and Buhl, R., Preparation etudes cristallines et magnetiques du manganite de nickel $NiMn_2O_4$. *C. R. Hebd. Seances Acad. Sci.*, 1965, **260**, 3406–3412.
24. Tang, X., Manthiram, A. and Goodenough, J. B., $NiMn_2O_4$ revisisted. *J. Less Common Met.*, 1989, **156**, 357–368.
25. Baudour, J. L. *et al.*, Cation distribution and oxidation states in nickel manganites $NiMn_2O_4$ and $Ni_{0.8}Mn_{2.2}O_4$. *Physica B*, 1992, **180–181**, 97–99.
26. Young, R. A., ed., *The Rietveld Method. IUCr Monographs on Crystallography, Vol 5* (*1st ed.*). Oxford University Press, Oxford, UK, 1993.
27. Drouet, C., Alphonse, P. and Rousset, A., Synthesis and characterisation of non-stoichiometric nickel copper manganites. *Solid State Ionics*, 1999, **123**, 25–37.
28. Boucher, B., Buhl, R. and Perrin, M., Structure magnetiques et etude des proprietes magnetiques des spinelles cubiques $NiMn_2O_4$. *J. Phys. Chem. Solids*, 1970, **31**, 363–383.
29. Shannon, R. D., Revised effective ionic radii and systematic studies of interatomic distances in halides and chalcogenides. *Acta Cryst. A*, 1976, **32**, 751–767.
30. O' Neill, H. S. C. and Navrotsky, A., Simple spinels: crystallographic parameters, cation radii, lattice energies, and cation distributions. *Am. Mineral.*, 1983, **68**, 181–194.
31. Brabers, V. A. M., Ionic ordering and infrared spectra of some II–IV spinels. *Phys. Status Solidi A*, 1972, **12**, 629–636.
32. Cervinka, L., A new parameter for description of cubic manganese ferrite spinel lattice. *J. Phys. Chem. Solids*, 1965, **26**, 1917–1923.
33. Brabers, V. A. M. and Terhell, J. C. J. M., Electrical conductivity and cation valences in nickel manganite. *Phys. Status Solidi A*, 1982, **69**, 325–332.
34. Topfer, J., Feltz, A., Graf, D., Hackl, B., Ranpach, L. and Weissbrodt, P., Cation valencies and distribution in the spinels $NiMn_2O_4$ and $M_zNiMn_{2-z}O_4$ (M = Li, Cu) studied by XPS. *Phys. Status Solidi A*, 1992, **134**, 405–415.